ACS Sustainable Chemistry & Engineering

Research Article

pubs.acs.org/journal/ascecg

Catalytic Conversion of Fructose and 5-Hydroxymethylfurfural into 2,5-Furandicarboxylic Acid over a Recyclable Fe_3O_4–CoO_x Magnetite Nanocatalyst

Shuguo Wang, Zehui Zhang,* and Bing Liu

Key Laboratory of Catalysis and Material Sciences of the State Ethnic Affairs Commission and Ministry of Education, South-Central University for Nationalities, Minyuan Road 182, Wuhan 430074, China

Supporting Information

ABSTRACT: A nano-Fe_3O_4–CoO_x catalyst was prepared via a simple wet impregnation method. The nano-Fe_3O_4–CoO_x catalyst showed good catalytic performance for the conversion of 5-hydroxymethylfurfural into 2,5-furandicarboxylic acid (FDCA) with *t*-BuOOH as the oxidant. Several important reaction parameters were explored, with the highest FDCA yield of 68.6% obtained from HMF after 15 h at a reaction temperature of 80 °C. One-pot conversion of fructose into FDCA was also successful via two steps. Catalytic conversion of fructose over Fe_3O_4@SiO_2–SO_3H yielded 93.1% HMF, which was oxidized in situ into FDCA with a yield of 59.8%. Furthermore, recycling of nano-Fe_3O_4–CoO_x was accomplished with the help of a magnetic field. Nano-Fe_3O_4–CoO_x showed high stability in the reaction process. The use of nonprecious metals and no requirement of a base additive made this method much more economical and environmentally friendly.

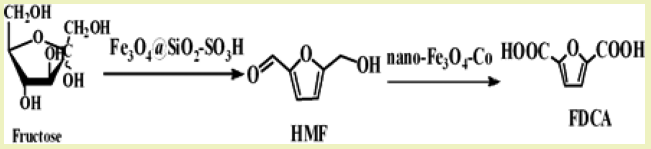

KEYWORDS: *Oxidation, 5-Hydroxymethylfurfural, 2, 5-Furandicarboxylic acid, Magnetite catalyst, Sustainable chemistry*

INTRODUCTION

Nanoparticles as catalysts have been extensively used in chemical reactions in recent years.[1,2] Although using a catalyst in nanometer dimensions may achieve a substantial enhancement in its catalytic activity, recycling of nanocatalysts is difficult, especially for large-scale processes. From the viewpoint of green chemistry, it is beneficial to develop new catalyst recycling methods to replace conventional procedures such as centrifugation and filtration. In this context, magnetite nanoparticles have been attracted much attention for various organic reactions.[3]

Magnetite nanoparticles possess high thermal and mechanical stability.[4] More importantly, their unique paramagnetic properties and inherent insolubility allow them to be efficiently separated from the reaction mixtures by a magnet. Furthermore, the minimal workup procedures required and the minimal amount of waste generated from their preparation adequately satisfy the requirements of green chemistry principles. In particular, magnetically recoverable catalysts have been well designed and extensively used in many chemical reactions including oxidation,[5] hydrogenation,[6] coupling reactions,[7] cycloaddition,[8] acylation,[9] photocatalysis,[10] and so forth.[11]

On the other hand, with limited fossil resources, the search for chemicals and fuels from renewable sources has recently attracted considerable interest.[12,13] Biomass is the only carbon containing renewable resource.[14−16] 5-Hydroxymethylfurfural (HMF) is regarded as a value-added platform chemical.[17−20] As shown in Scheme 1, several important furan chemicals can be obtained by the oxidation of HMF including 5-hydroxymethyl-2-furancarboxylic acid (HMFCA),[21] 2,5-diformylfuran (DFF), and FDCA.[22,23] In contrast to HMFCA and DFF, FDCA has received a great deal of attention as an excellent candidate as a monomer for the synthesis of polymers.[24] FDCA has the ability to replace terephthalic acid in the synthesis of polyamides, polyesters, and polyurethanes.[25]

Scheme 1. Catalytic Oxidation Products of HMF

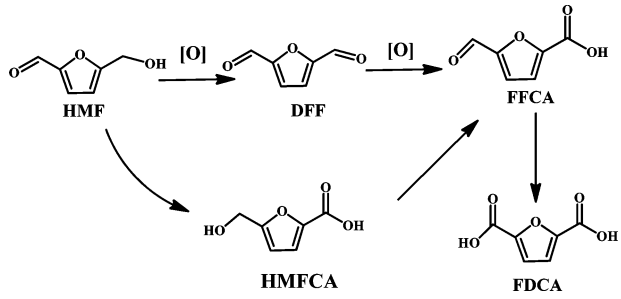

There are many reports on the oxidation of HMF into FDCA. In one such report, homogeneous metal acetate catalysts including $Co(OAc)_2$, $Mn(OAc)_2$, and HBr were applied for the synthesis of FDCA from HMF at 70 bar air pressure in acetic acid.[26] Recently, a similar reaction system was also developed for the transformation of HMF into FDCA in the presence of homogeneous catalysts [$Co(OAc)_2$/$Zn(OAc)_2$/NaBr].[27] However, it is difficult to recycle homoge-

Received: August 14, 2014
Revised: January 2, 2015
Published: January 7, 2015

DOI: 10.1021/sc500702q
ACS Sustainable Chem. Eng. 2015, 3, 406−412

neous catalysts. Recently, heterogeneous catalysts have been widely utilized for chemical reactions.[28] Among various heterogeneous catalysts, supported gold nanoparticles have been extensively used for the oxidation of HMF into FDCA.[29−31] Although some of the reported methods produced high FDCA yields, some drawbacks were still present, including the high cost of the noble catalyst, high oxygen pressure, and use of base additives.

Transition metal-based heterogeneous catalysts have triggered much interest due to their low cost. It is reported that cobalt-based heterogeneous catalysts demonstrated high catalytic activity in alcohol oxidations.[32] Herein, magnetite Fe_3O_4 nanoparticles were used to support Co nanoparticles to construct a nano-Fe_3O_4−Co catalyst that was employed for the synthesis of FDCA from HMF.

EXPERIMENTAL SECTION

Catalyst Preparation. The procedure for the preparation of the nano-Fe_3O_4−CoO_x catalyst followed those outlined in published references.[33,34] $FeCl_3{\cdot}6H_2O$ (5.4 g) and urea (3.6 g) were added to deionized water (200 mL) at 90 °C and stirred vigorously for 2 h. The mixture was then cooled to room temperature and $FeSO_4{\cdot}7H_2O$ (2.8 g) was added. Finally, 0.1 M NaOH solution was added dropwise to adjust the pH to 10. The slurry was subjected to ultrasound at room temperature for 30 min, after which the mixture was aged for 5 h. Fe_3O_4 nanoparticles were washed with water and dried in a vacuum oven.

Fe_3O_4 nanoparticles (2.0 g) and $CoCl_2.6H_2O$ (0.6 g) were added into water (50 mL) and stirred at 25 °C for 1 h. Then NaOH (0.5 M) was added dropwise until the pH value of the suspension reached 12. The suspension was then stirred for 12 h, and the precipitate was washed with deionized water. Next, the Co^{2+} on the surface of the Fe_3O_4 nanoparticles was treated with 0.2 M aqueous $NaBH_4$ at 0 °C until no gas was bubbled from the solution. Nano-Fe_3O_4−CoO_x nanoparticles were treated under ultrasonication for 10 min and then purified with the eluent of water and ethanol in sequence. Finally, the as-prepared catalyst was dried under vacuum at 60 °C for 24 h.

Catalyst Characterization. An FEI Tecnai G^2-20 instrument was used to collect transmission electron microscope (TEM) images. The catalyst dispersed in ethanol was disposed onto copper grids for the TEM test. X-ray powder diffraction (XRD) was performed on samples using a Bruker advanced D8 powder diffractometer (Cu Kα). A scanning rate of 0.016°/s was employed in the 2θ range of 10−80°. Thermo VG scientific ESCA multiLab-2000 spectrometer X-ray photoelectron spectroscopy (XPS) was performed with a monochromatized Al Kα source (1486.6 eV) at a constant analyzer pass energy of 25 eV. All binding energies (BEs) were corrected based on the C 1s (284.6 eV) peak of the contamination carbon as an internal standard. The weight percentage of Co was determined by atomic absorption spectroscopy (AA-6300, Shimadzu).

Catalytic Conversion of HMF into FDCA. HMF (70 mg), 70% aqueous TBHP (0.5 mL), and Fe_3O_4−CoO_x (100 mg) were added into dimethyl sulfoxide (DMSO) (4 mL) and then stirred at 80 °C for the desired reaction time. After the reaction, the nano-Fe_3O_4−CoO_x catalyst was collected using the force of a magnetic field, and furan compounds in the liquid solution were quantified on an HPLC device.

Quantitative Determination of the Products Methods. A ProStar 210 HPLC system was used for the quantitative determination of furan compounds. The furan compounds showed high resolution using a reversed-phase C18 column (200 mm × 4.6 mm) at a wavelength of 280 nm. The mobile phase consisted of acetonitrile and 0.1 wt % acetic acid aqueous solution (v/v = 30:70). The eluent was washed at a rate of 1.0 mL/min. Interpolation from calibration curves was applied to calculate the amount of HMF and FDCA in the samples.

RESULTS AND DISCUSSION

Characterization of Catalyst. Scheme 2 shows the method of the nano-Fe_3O_4−CoO_x catalyst preparation.

Scheme 2. Schematic of Nano-Fe_3O_4−CoO_x Catalyst Preparation

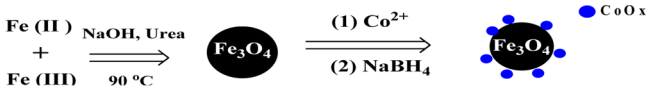

Magnetite Fe_3O_4 nanoparticles were easily prepared by the coprecipitation of Fe^{3+} and Fe^{2+} in a strong alkaline solution. Then Fe_3O_4 nanoparticles were impregnated with the $CoCl_2$ solution, followed by chemical reduction to produce the nano-Fe_3O_4−CoO_x catalyst. The content of Co in the catalyst was determined to be 6.95 wt % by atomic absorption spectroscopy.

Figure 1 shows the TEM image of the nano-Fe_3O_4−CoO_x nanoparticles. Magnetite Fe_3O_4−CoO_x nanoparticles were

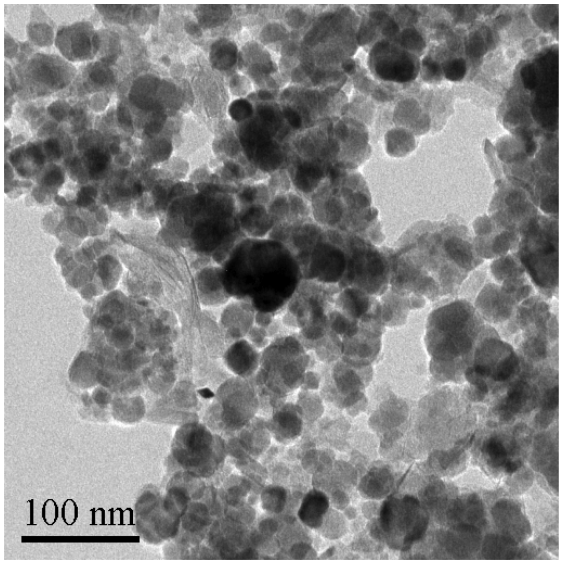

Figure 1. TEM image of the nano-Fe_3O_4−CoO_x catalyst.

observed to be of spherical morphology with nanosize range. However, some aggregations/coalescences of individual Fe_3O_4−CoO_x nanoparticles were also observed.

The crystallinity and phase composition of the nano-Fe_3O_4−CoO_x catalyst were characterized by XRD technology. XRD spectra of nano-Fe_3O_4−CoO_x catalyst is presented in Figure 2. The sharp and strong peaks confirmed that the catalyst was well crystallized. Six characteristic diffraction peaks with 2θ = 30.2°, 35.6°, 43.3°, 53.8°, 57.3°, and 63.0° were attributed to (220), (311), (400), (422), (511), and (440), respectively, of Fe_3O_4 (JCPDS No. 19-0629).[35] However, there was no diffraction peak for Co species, possibly due to fact that Co species in small size were homogeneously dispersed on the surface of the Fe_3O_4 nanoparticles.

The XPS spectrum of the nano-Fe_3O_4−CoO_x catalyst is shown in Figure 3. The survey spectrum gives signals mainly associated with Co 3p, O 1s, Fe 2p, and Co 2p species, indicating that the nano-Fe_3O_4−CoO_x catalyst was composed of Co, O, and Fe elements. Two peaks at 710.9 and 724.5 eV were assigned to Fe $2p_{3/2}$ and Fe $2p_{1/2}$, respectively, which represent the characteristic peaks of Fe^{2+} in Fe_3O_4. This is in

DOI: 10.1021/sc500702q
ACS Sustainable Chem. Eng. 2015, 3, 406−412

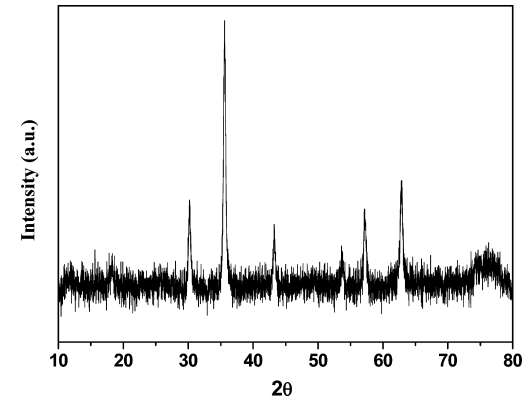

Figure 2. XRD patterns of the nano-Fe_3O_4−CoO_x catalyst.

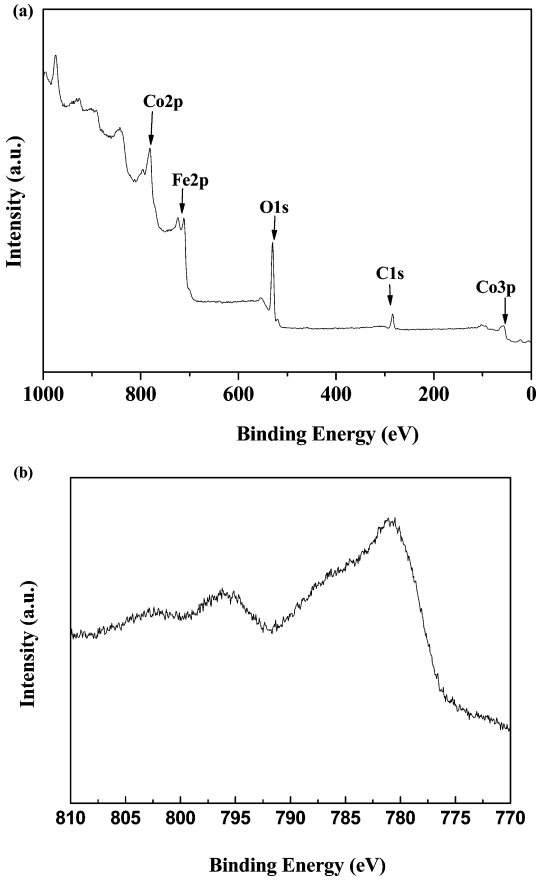

Figure 3. XPS spectra of the nano-Fe_3O_4−CoO_x catalyst. (a) Survey scan of nano-Fe_3O_4- CoO_x and (b) Co 2p region.

agreement with the reported results for the magnetite Fe_3O_4.[35] As shown in Figure 3b, two peaks at 780.8 and 796.3 eV were also present and were assigned to Co 2p3/2 and Co 2p1/2 peaks, respectively. In addition, both peaks are accompanied by broad shakeup satellites located approximately 6.5 eV above the primary BE peak. It is not easy to determine the Co valence state, and it is reported that CoO or Co_3O_4 show similar Co 2p spectra.[36] The energy gap between the main peak and satellites can be applied to detect the valence state of Co. If the satellites are located about 6 eV above the primary BE peak, the spectra is usually attributed to Co^{2+}. In contrast, if the satellites are located about 10 eV above the primary BE peak, the peak is usually attributed to Co_3O_4.[37] As shown in Figure 3b, it is observed that Co 2p was present in combination with a small satellite peak. In addition, an approximate shift of about 6.5 eV revealed that the valence state of Co was +2 and in the form of CoO. Although Co^{2+} was reduced to a Co(0) nanoparticle by $NaBH_4$ during the catalyst preparation, it was oxidized to a high valence state species. It is reported that metal nanoparticles are active and sensitive to oxygen. For instance, it has been reported that metallic Ru was transformed into a high oxidation state when exposed to oxygen during storage.[38]

The results of the oxidation of HMF by various oxidants. Initially, three common oxidants including O_2, H_2O_2, and *t*-BuOOH were used for the oxidation of HMF over the nano-Fe_3O_4−CoO_x catalyst. Poor results were obtained when using O_2 and H_2O_2 as oxidants (Table 1, entries 1 and 2).

Table 1. Catalytic Conversion of HMF into FDCA Using Various Oxidants[a]

entry	oxidant	time (h)	HMF conversion (%)	FDCA yield (%)	DFF yield (%)
1[b]	O_2	12	13.4	4.2	6.6
2[c]	H_2O_2	12	9.0	1.0	1.3
3[d]	*t*-BuOOH	12	97.2	68.6	7.7

[a]Reaction conditions: nano-Fe_3O_4−CoO_x (100 mg), HMF (70 mg), 80 °C, and DMSO (4 mL). [b]Flow rate of O_2 was 20 mL min^{-1}. [c]1 mL of H_2O_2 was used. [d]0.5 mL of 70% aqueous *t*-BuOOH was used.

In addition, oxygen was produced after the addition of H_2O_2, suggesting nano-Fe_3O_4−CoO_x catalyzed the decomposition of H_2O_2 into O_2. In fact, Co species have showed catalytic activity in the transformation of H_2O_2 into O_2.[39] Therefore, the use of H_2O_2 was not suitable for this kind of reaction over the nano-Fe_3O_4−CoO_x catalyst due to the decomposition of H_2O_2 (Table 1, entry 2). Among the three oxidants, 70% aqueous *t*-BuOOH gave the best results (Table 1, entry 3). Besides O_2 and H_2O_2, the use of *t*-BuOOH as the oxidant has also been popular in oxidation reactions. In our reactions, the mole ratio of *t*-BuOOH to HMF was close to 7, which seemed a little high. In fact, the oxidation of one HMF molecule into one FDCA molecule required three *t*-BuOOH molecules based on the electron transfer in the redox reaction. After the reaction, the amount of *t*-BuOOH remaining in the reaction solution was determined to be 34.2% of the starting *t*-BuOOH. This value is a little lower than the theoretical value (57.1% of the starting *t*-BuOOH), which could be caused by the decomposition of *t*-BuOOH into other products during the reaction process.

Catalytic Oxidation of HMF into FDCA with *t*-BuOOH in Various Solvents. Generally speaking, the efficiency of chemical reactions is greatly affected by the reaction solvent, as each solvent has different polarities, dielectric constants, steric hindrance factors, and acid−base properties.[40] Therefore, the effect of the solvent on this reaction was studied. H_2O is the most preferable solvent in terms of sustainable chemistry but produced a low HMF conversion of 48.3% and FDCA yield of 10.7% (Table 2, entry 1). The lowest HMF conversion and FDCA yield were obtained in protic ethanol with low boiling point (Table 2, entry 2). Although a high conversion of 94.2% was reached in low boiling point aprotic acetonitrile (CH_3CN), the selectivity of FDCA was only 45.6% (Table 2, entry 3). HMF conversion reached 98.7% in methyl isobutyl ketone (MIBK) but gave a low FDCA yield of 32.1% (Table 2, entry 4). The best results were achieved in DMSO (Table 2, entry 5), which generated FDCA in a yield of 68.6%. In our reaction

DOI: 10.1021/sc500702q
ACS Sustainable Chem. Eng. 2015, 3, 406−412

Table 2. Effect of Solvent on Oxidation of HMF[a]

entry	solvent	time (h)	HMF conversion (%)	FDCA yield (%)	DFF yield (%)	FDCA selectivity (%)
1	H_2O	12	48.3	10.7	4.4	22.1
2	ethanol	12	11.4	6.3	2.1	55.3
3	CH_3CN	12	94.2	43.0	18.2	45.6
4	MIBK	12	83.4	32.1	10.4	38.5
5	DMSO	12	97.2	68.6	7.7	70.6
6[b]	DMSO	12	8.5	0.5	1.3	0
7[c]	DMSO	12	13.2	1.0	2.4	0

[a]Reaction conditions: Fe_3O_4−CoO_x (100 mg), HMF (70 mg), 80 °C, 70% aqueous *t*-BuOOH (0.5 mL), and solvent (4 mL). [b]No catalyst was used. [c]Fe_3O_4 was used for this reaction.

system, DFF, FDCA, and very little HMFCA were determined as the oxidation products for all the cases, and there were no other furans compounds. This indicated that HMF degradation such as the ring opening of the furan ring occurred during the oxidation process in all solvents. Reactions were also performed without a catalyst or with Fe_3O_4. Low HMF conversions and products yield were obtained (Table 2, entries 6 and 7). Comparing the results in entries 6 and 7 with those in entry 5, it can be concluded that the Co species were the active center for this reaction.

Catalytic Conversion of HMF at Various Temperatures. The good results at 80 °C prompted us to perform this reaction at lower reaction temperatures of 60 and 25 °C. As depicted in Table 3, the oxidation of HMF was greatly

Table 3. Effect of Reaction Temperature on Conversion of HMF[a]

entry	temperature (°C)	time (h)	HMF conversion (%)	FDCA yield (%)	DFF yield (%)
1	80	12	97.2	68.6	7.7
2	60	12	48.5	19.3	19.8
3	25	12	8.0	2.6	4.2
4	100	6	99.5	25.7	2.4
5	100	12	100	26.1	1.5

[a]Reaction conditions: nano-Fe_3O_4−CoO_x (100 mg), HMF (70 mg), 70% aqueous *t*-BuOOH (0.5 mL), and DMSO (4 mL).

influenced by the reaction temperature. Compared with the results obtained at 80 °C, a lower HMF conversion of 48.5% was obtained at 60 °C with a FDCA yield of 19.3% (Table 3, entry 1 vs 2), suggesting that the catalytic activity of nano-Fe_3O_4−CoO_x decreased by decreasing the reaction temperature. As expected, HMF conversion further decreased to 8.0% at 25 °C (Table 3, entry 3). FDCA and DFF were the main oxidation products at all three reaction temperatures (Table 3, entries 1−3). Compared with the results obtained at 25, 60, and 80 °C, the selectivity of FDCA was improved by increasing the reaction temperature, while the trend was opposite for DFF selectivity (Table 3, entries 1−3). The reason is likely that DFF was the intermediate for the conversion of HMF into FDCA. In addition, it was also found that the total selectivity of DFF and FDCA increased with a decrease in reaction temperature (Table 3, entries 1−3), which indicated that many more side reactions occurred at higher reaction temperatures. For comparison, the reaction was also performed at 100 °C. It only needed 6 h to get 99.5% conversion of HMF, but the yield of FDCA was only 25.7% (Table 3, entry 4). Interestingly, FDCA yield was almost the same after 12 h (Table 3, entry 4 vs 5).

Products Concentration during Oxidation of HMF into FDCA. Figure 4 presents the concentration of each

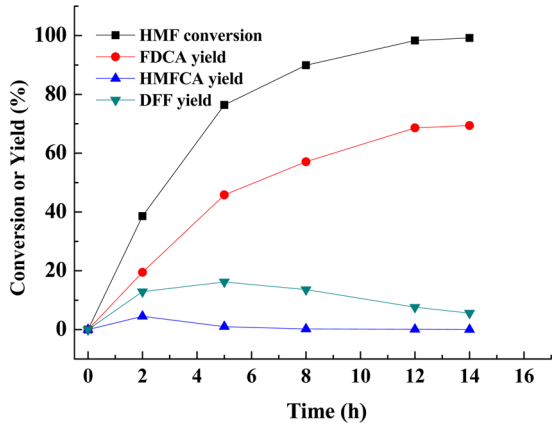

Figure 4. Products analysis during the procedure of the oxidation of HMF. Reaction conditions: HMF (70 mg), nano-Fe_3O_4−CoO_x (100 mg), 70% aqueous *t*-BuOOH (0.5 mL), DMSO (4 mL), and 80 °C.

product at different reaction time points. HMF conversion increased gradually during the reaction process. It is worth noting that the increasing trend of HMF conversion was sharp in the initial 5 h due to the high concentration of HMF at an early reaction stage. Then, it slowly increased from 75.2% at 5 h to 100% after 15 h. The FDCA yield also increased gradually during the reaction process, and the maximum FDCA yield of 69.4% was achieved after 15 h. Other oxidation products including DFF and HMFCA were also detected and were believed to be the intermediates. The DFF yield and HMFCA yield first increased at an early reaction stage and then decreased gradually at the late reaction stage. These results confirmed that DFF and HMFCA were both the intermediates in the transformation of HMF into FDCA, which suggested that both the hydroxyl group and the aldehyde group in HMF could be simultaneously oxidized in the first step (Scheme 3).

Scheme 3. Possible Catalytic Routes for Conversion of HMF into FDCA over Nano-Fe_3O_4−CoO_x Catalyst

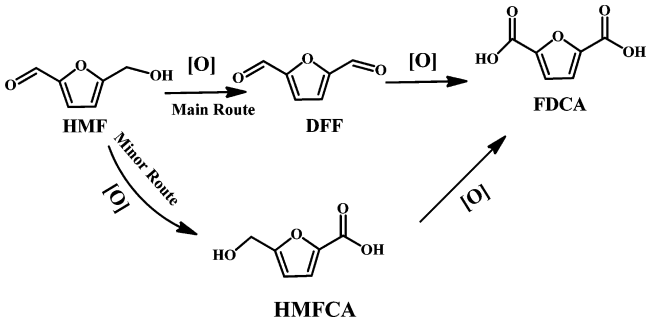

However, as shown in Figure 2, DFF yield was much higher than HMFCA yield, which indicated that oxidation of the hydroxyl group in HMF was the main reaction. According to the above results, reasonable routes for the transformation of HMF into FDCA over the Fe_3O_4−Co catalyst were proposed in Scheme 3.

DOI: 10.1021/sc500702q
ACS Sustainable Chem. Eng. 2015, 3, 406−412

Scheme 4. Conversion of Fructose into FDCA from Fructose via Two Steps

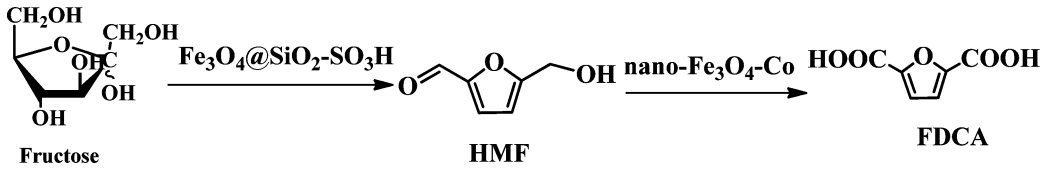

Synthesis of FDCA from Fructose via Two Consecutive Steps. Finally, the one-pot conversion of fructose into FDCA was studied. Fe_3O_4@SiO_2−SO_3H was used as the acid catalyst with the aim of the facile separation of the reaction solution. Synthesis and characterization of Fe_3O_4@SiO_2−SO_3H were described elsewhere in our previous work.[41] Initially, synthesis of FDCA from fructose by a one-pot reaction method was applied, in which Fe_3O_4@SiO_2−SO_3H catalyzed the dehydration reaction and the nano-Fe_3O_4−CoO_x catalyst promoted the oxidation reaction. Unfortunately, this method produced HMF and DFF at low yields of 5.3% and 2.6%, respectively. This may be caused by the possible oxidation of fructose, resulting in other undesired byproducts.[42]

Therefore, two consecutive steps (Scheme 4) were used for the synthesis of FDCA from fructose. HMF was first produced from fructose over the Fe_3O_4@SiO_2−SO_3H catalyst. As shown in Figure 5, dehydration of fructose proceeded fast in a short reaction time, with HMF reaching a maximum yield of 93.1% after 2 h at 100 °C. The Fe_3O_4@SiO_2−SO_3H catalyst was then magnetically collected, and the nano-Fe_3O_4−CoO_x and 70% aqueous *t*-BuOOH were added into the liquid solution. The following reaction was carried out at 80 °C. As depicted in Figure 5, FDCA was obtained in a yield of 59.8% after 15 h based on the starting fructose. Other methods were also used for the synthesis of FDCA from fructose. Kröger et al. also reported two steps for the production of FDCA from fructose.[43] In the first step, the dehydration of fructose generated HMF, which was extracted from the reaction solution by MIBK. Then PtBi/C catalyzed the subsequent oxidation reaction. The total yield of FDCA by Kröger et al. was lower than that obtained by our method.[43] In addition, this method required using MIBK as the second solvent and the use of a noble metal catalyst. Thus, the cost of this method is higher than our method and is not economical for the production of FDCA from fructose. Ribeiro and co-workers also reported the conversion of fructose into FDCA by a cobalt catalyst, in which fructose conversion reached 72% with FDCA selectivity of 99%.[44] The cost of this method was lower than that by Kröger et al.[43] However, it was carried out under harsh conditions at a high reaction temperature of 160 °C and at 20 bar air pressure.

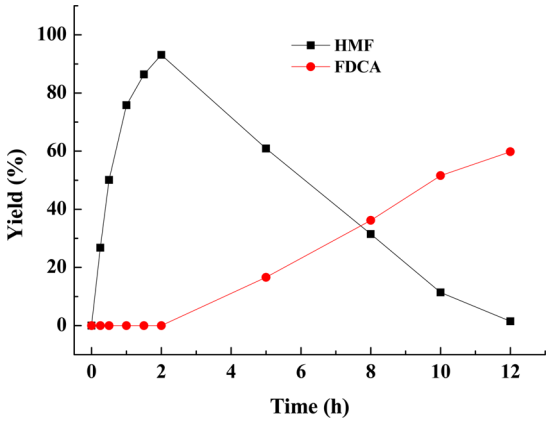

Figure 5. Synthesis of FDCA from fructose via two-step method. Reaction conditions for the first step: Fructose (100 mg) and Fe_3O_4@SiO_2−SO_3H (150 mg) were added into DMSO (4 mL), and the mixture was carried out at 100 °C. Reaction conditions for the second step: Nano-Fe_3O_4−CoO_x (100 mg) and 70% aqueous *t*-BuOOH (0.5 mL) were added into the reaction solution, and the mixture was stirred at 80 °C.

Study of Stability of the Catalyst. Finally, the stability of nano-Fe_3O_4−CoO_x was studied. Synthesis of FDCA from HMF at 80 °C was used as the mode reaction. After the reaction, the nano-Fe_3O_4−CoO_x catalyst was dispersed in the reaction solution (Figure S1 a, Supporting Information), but it was quickly collected on the side of the bottle with the assistance of an external magnet (Figure S1 b, Supporting Information). The nano-Fe_3O_4−CoO_x catalyst was washed three times with water and then dried in a vacuum oven at 50 °C for 12 h. Then, the recovered nano-Fe_3O_4−CoO_x was reused in the second run under the same reaction conditions as the first cycle. FDCA yields in the subsequent cycles were almost the same as in the first cycle (Figure S2, Supporting Information) suggesting that the catalytic activity of nano-Fe_3O_4−CoO_x showed no significant decrease. In addition, the reaction solution was analyzed by atomic absorption spectroscopy, and no Co species were found to remain in the reaction solution, indicating that there was no leaching of the active site Co during the reaction process.

CONCLUSIONS

The nano-Fe_3O_4−CoO_x catalyst showed high catalytic activity in the oxidation of HMF into FDCA with *t*-BuOOH as the oxidant. The highest FDCA yield of 68.4% was obtained after 12 h at 80 °C in DMSO. The one-pot conversion of fructose into FDCA was also successfully realized via two consecutive steps with the total FDCA yield reaching 59.8%. The Fe_3O_4−CoO_x catalyst was also magnetically separable, and its catalytic activity showed no significant loss during the recycling experiments.

ASSOCIATED CONTENT

Supporting Information

Separation of the catalyst simply by a magnet and the recycle results. This material is available free of charge via the Internet at http://pubs.acs.org.

AUTHOR INFORMATION

Corresponding Author

*Fax: +8627-67842752. Tel: +8627-67842752. E-mail: zehuizh@mail.ustc.edu.cn.

Notes

The authors declare no competing financial interest.

DOI: 10.1021/sc500702q
ACS Sustainable Chem. Eng. 2015, 3, 406−412

■ ACKNOWLEDGMENTS

The project was supported by the National Natural Science Foundation of China (21203252). The authors thank Kevin Barnett, Ph.D., for his help in improving the English.

■ REFERENCES

(1) Gawande, M. B.; Branco, P. S.; Varma, R. S. Nano-magnetite (Fe_3O_4) as a support for recyclable catalysts in the development of sustainable methodologies. *Chem. Soc. Rev.* **2013**, *42*, 3371−3393.
(2) Wang, D.; Astruc, D. Fast-growing field of magnetically recyclable nanocatalysts. *Chem. Rev.* **2014**, *114*, 6949−6985.
(3) Lu, A. H.; Salabas, E. L.; Schuth, F. A practical heterogeneous catalyst for the Suzuki, Sonogashira, And Stille coupling reactions of unreactive aryl chlorides. *Angew. Chem., Int. Ed.* **2007**, *46*, 1222−1244.
(4) Gawande, M. B.; Branco, P. S.; Nogueira, I. D.; Ghumman, C. A. A.; Bundaleski, N.; Santos, A.; Teodoro, O. M. N. D.; Luque, R. Catalytic applications of a versatile magnetically separable Fe−Mo (Nanocat-Fe−Mo) nanocatalyst. *Green Chem.* **2013**, *15*, 682−689.
(5) Zhang, Z. H.; Yuan, Z. L.; Tang, D. G.; Ren, Y. S.; Lv, K. L.; Liu, B. Iron oxide encapsulated by ruthenium hydroxyapatite as heterogeneous catalyst for the synthesis of 2,5-diformylfuran. *ChemSusChem* **2014**, *7*, 3496−3504.
(6) Gawande, M. B.; Rathi, A. K.; Branco, P. S.; Nogueira, I. D.; Velhinho, A.; Shrikhande, J. J.; Indulkar, U. U.; Jayaram, R. V.; Ghumman, C. A. A.; Bundaleski, N. Regio- and chemoselective reduction of nitroarenes and carbonyl compounds over recyclable magnetic ferrite−nickel nanoparticles (Fe_3O_4−Ni) by using glycerol as a hydrogen source. *Chem.—Eur. J.* **2012**, *18*, 12628−12632.
(7) Luque, R.; Baruwati, B.; Varma, R. S. Magnetically separable nanoferrite-anchored glutathione: Aqueous homocoupling of arylboronic acids under microwave irradiation. *Green Chem.* **2010**, *12*, 1540−1543.
(8) Wang, D.; Salmon, L.; Ruiz, J.; Astruc, D. A recyclable ruthenium(II) complex supported on magnetic nanoparticles: A regioselective catalyst for alkyne−azide cycloaddition. *Chem. Commun.* **2013**, *49*, 6956−6958.
(9) Parella, R.; Naveen, A. K.; Babu, S. A. Catalytic Friedel−Crafts acylation: Magnetic nanopowder $CuFe_2O_4$ as an efficient and magnetically separable catalyst. *Tetrahedron Lett.* **2013**, *54*, 1738−1742.
(10) Alamo-Nole, L.; Bailon-Ruiz, S.; Luna-Pineda, T.; Perales-Perez, O.; Roman, F. R. Photocatalytic activity of quantum dot−magnetite nanocomposites to degrade organic dyes in the aqueous phase. *J. Mater. Chem. A* **2013**, *1*, 5509−5516.
(11) Wang, S. G.; Zhang, Z. H.; Liu, B.; Fang, Z. F.; Li, J. L. Environmentally friendly oxidation of biomass derived 5-hydroxymethylfurfural into 2,5-diformylfuran catalyzed by magnetic separation of ruthenium catalyst. *Ind. Eng. Chem. Res.* **2014**, *53*, 5820−5827.
(12) Zhang, J. F.; Chen, Y.; Brook, M. A. Reductive degradation of lignin and model compounds by hydrosilanes. *ACS Sustainable Chem. Eng.* **2014**, *2*, 1983−1991.
(13) Christodoulou, C.; Grimekis, D.; Panopoulos, K. D.; Vamvuka, D.; Karellas, S.; Kakaras, E. Circulating fluidized bed gasification tests of seed cakes residues after oil extraction and comparison with wood. *Fuel* **2014**, *132*, 71−81.
(14) Liu, A.; Liu, B.; Wang, Y.; Ren, R.; Zhang, Z. H. Efficient conversion of carbohydrates into 5-ethoxymethylfurfural in ethanol catalyzed by $AlCl_3$. *Fuel* **2014**, *117*, 68−73.
(15) Besson, M.; Gallezot, P.; Pinel, C. Conversion of biomass into chemicals over metal catalysts. *Chem. Rev.* **2014**, *114*, 1827−1870.
(16) Xiong, Y.; Zhang, Z. H.; Wang, X.; Liu, B.; Lin, J. Hydrolysis of cellulose in ionic liquids catalyzed by a magnetically-recoverable solid acid catalyst. *Chem. Eng. J.* **2014**, *235*, 349−355.
(17) Jadhav, A. H.; Chinnappan, A.; Patil, R. H.; Kostjuk, S. V.; Kim, H. Green chemical conversion of fructose into 5-hydroxymethylfurfural (HMF) using unsymmetrical dicationic ionic liquids under mild reaction condition. *Chem. Eng. J.* **2014**, *243*, 92−98.
(18) Liu, B.; Zhang, Z. H. One-pot conversion of carbohydrates into 5-ethoxymethylfurfural and ethyl glucoside in ethanol catalyzed by silica supported sulfonic acid catalyst. *RSC Adv.* **2013**, *3*, 12313−12319.
(19) Xiao, S.; Liu, B.; Wang, Y.; Fang, Z.; Zhang, Z. Efficient conversion of cellulose into biofuel precursor 5-hydroxymethylfurfural in dimethyl sulfoxide-ionic liquid mixtures. *Bioresour. Technol.* **2014**, *151*, 361−366.
(20) van Putten, R. J.; van der Waal, J. C.; de Jong, E.; Rasrendra, C. B.; Heeres, H. J.; de Vries, J. G. Hydroxymethylfurfural, a versatile platform chemical made from renewable resources. *Chem. Rev.* **2013**, *113*, 1499−597.
(21) Zhang, Z. H.; Liu, B.; Lv, K. L.; Sun, J.; Deng, K. J. Aerobic oxidation of biomass derived 5-hydroxymethylfurfural into 5-hydroxymethyl-2-furancarboxylic acid (HMFCA) catalyzed by montmorillonite K-10 clay immobilized molybdenum acetylacetonate complex. *Green Chem.* **2014**, *16*, 2762−2770.
(22) Takagaki, A.; Takahashi, M.; Nishimura, S.; Ebitani, K. One-pot Synthesis of 2,5-diformylfuran from carbohydrate derivatives by sulfonated resin and hydrotalcite-supported ruthenium catalysts. *ACS Catal.* **2011**, *1*, 1562−1565.
(23) Zhang, Z. H.; Yuan, Z. L.; Tang, D. G.; Ren, Y. S.; Lv, K. L.; Liu, B. Iron oxide encapsulated by ruthenium hydroxyapatite as heterogeneous catalyst for the synthesis of 2,5-diformylfuran. *ChemSusChem* **2014**, *7*, 3496−3504.
(24) Zhou, W.; Wang, X.; Yang, X.; Xu, Y.; Zhang, W.; Zhang, Y.; Ji, J. Synthesis, physical properties and enzymatic degradation of bio-based poly(butylene adipate-co-butylene furandicarboxylate) copolyesters. *Polym. Degrad. Stab.* **2013**, *106*, 2177−2183.
(25) Moreau, C.; Belgacem, M. N.; Gandini, A. Recent catalytic advances in the chemistry of substituted furans from carbohydrates and in the ensuing polymers. *Top. Catal.* **2004**, *27*, 11−30.
(26) Partenheimer, W.; Grushin, V. V. Synthesis of 2,5-diformylfuran and furan-2,5-dicarboxylic acid by catalytic air-Oxidation of 5-hydroxymethylfurfural. unexpectedly selective aerobic oxidation of benzyl alcohol to benzaldehyde with metal−bromide catalysts. *Adv. Synth. Catal.* **2001**, *343*, 102−111.
(27) Saha, B.; Dutta, S.; Abu-Omar, M. M. Aerobic oxidation of 5-hydroxylmethylfurfural with homogeneous and nanoparticulate catalysts. *Catal. Sci. Technol.* **2012**, *2*, 79−81.
(28) Liu, B.; Ren, Y. S.; Zhang, Z. H. Aerobic oxidation of 5-hydroxymethylfurfural into 2,5-furandicarboxylic acid in water under mild conditions. *Green Chem.* **2015**, DOI: 10.1039/c4gc02019g.
(29) Gupta, N. K.; Nishimura, S.; Takagaki, A.; Ebitani, K. Hydrotalcite-supported gold-nanoparticle-catalyzed highly efficient base-free aqueous oxidation of 5-hydroxymethylfurfural into 2,5-furandicarboxylic acid under atmospheric oxygen pressure. *Green Chem.* **2011**, *13*, 824−827.
(30) Zhang, Z. H.; Zhen, J. D.; Liu, B.; Lv, K. L.; Deng, K. J. Selective aerobic oxidation of biomass derived precursor 5-hydroxymethylfurfural into 2,5-furandicarboxylic acid under mild conditions over a magnetic palladium nanocatalyst. *Green Chem.* **2015**, DOI: 10.1039/c4gc01833h.
(31) Casanova, O.; Iborra, S.; Corma, A. Biomass into chemicals: Aerobic oxidation of 5-hydroxymethyl-2-furfural into 2,5-furandicarboxylic acid with gold nanoparticle catalysts. *ChemSusChem* **2009**, *2*, 1138−1144.
(32) Sharma, V. B.; Jain, S. L.; Sain, B. Cobalt (II) Schiff base catalyzed aerobic oxidation of secondary alcohols to ketones. *J. Mol. Catal. A* **2004**, *212*, 55−59.
(33) Gawande, M. B.; Rathi, A.; Nogueira, I. D.; Ghumman, C. A. A.; Bundaleski, N.; Teodoro, O. M. N. D.; Branco, P. S. A recyclable ferrite−Co magnetic nanocatalyst for the oxidation of alcohols to carbonyl compounds. *ChemPlusChem.* **2012**, *77*, 865−871.
(34) Dang, T.; Le, T.; Fribourg-Blanc, E.; Dang, M. C. Synthesis and optical properties of copper nanoparticles prepared by a chemical reduction method. *Adv. Nat. Sci.: Nanosci. Nanotechnol.* **2011**, *2*, 015009.

DOI: 10.1021/sc500702q
ACS Sustainable Chem. Eng. 2015, 3, 406−412

(35) Liu, B.; Zhang, Z. H.; Lv, K. L.; Deng, K. J.; Duan, H. M. Efficient aerobic oxidation of biomass-derived 5-hydromethylfurfural to 2,5-diformylfuran catalyzed by magnetic nanoparticle supported manganese oxide. *Appl. Catal., A* **2014**, *472*, 64−71.
(36) McIntyre, N. S.; Cook, M. G. X-ray photoelectron studies on some oxides and hydroxides of cobalt, nickel, and copper. *Anal. Chem.* **1975**, *47*, 2208−2213.
(37) Burriel, M.; Garcia, G.; Santiso, J.; Abrutis, A.; Saltyte, Z.; Figueras, A. Growth kinetics, composition, and morphology of Co_3O_4 thin films prepared by pulsed liquid-injection MOCVD. *Chem. Vap. Deposition* **2005**, *11*, 106−111.
(38) Liu, B.; Huang, T.; Zhang, Z. H.; Zhang, Y. H.; Wang, Z.; Li, J. L. The effect of the alkali additive on the highly active Ru/C catalyst for water gas shift reaction. *Catal. Sci. Technol.* **2014**, *4*, 1286−1292.
(39) Makhlouf, M. T.; Abu-Zied, B. M.; Mansoure, T. H. Effect of calcination temperature on the H_2O_2 decomposition activity of nanocrystalline Co_3O_4 prepared by combustion method. *Appl. Surf. Sci.* **2013**, *274*, 45−52.
(40) Sever, R. R.; Root, T. W. DFT study of solvent coordination effects on titanium-based epoxidation catalysts. part one: formation of the titanium hydroperoxo intermediate. *J. Phys. Chem. B* **2003**, *107*, 4080−4089.
(41) Zhang, Z. H.; Wang, Y. M.; Fang, Z. F.; Liu, B. Efficient synthesis of 5-ethoxymethylfurfural from fructose and inulin catalyzed by a novel magnetically-recoverable acid catalyst. *ChemPlusChem.* **2014**, *2*, 233−240.
(42) Heinen, A. W.; Peters, J. A.; van Bekkum, H. The oxidation of fructose on Pt/C catalysts. The formation of d-threo-hexo-2,5-diulose and the effect of additives. *Carbohydr. Res.* **1997**, *304*, 155−164.
(43) Kroger, M.; Prusse, U.; Vorlop, K. D. A new approach for the production of 2,5-furandicarboxylic acid by in situ oxidation of 5-hydroxymethylfurfural starting from fructose. *Top. Catal.* **2000**, *13*, 237−242.
(44) Ribeiro, M. L.; Schuchardt, U. Cooperative effect of cobalt acetylacetonate and silica in the catalytic cyclization and oxidation of fructose to 2,5-furandicarboxylic acid. *Catal. Commun.* **2003**, *4*, 83−86.

DOI: 10.1021/sc500702q
ACS Sustainable Chem. Eng. 2015, 3, 406−412